Trends in tuna carbon isotopes suggest global changes in pelagic phytoplankton communities

Anne Lorrain, Heidi Pethybridge, Nicolas Cassar, Aurore Receveur, Valérie Allain, Nathalie Bodin, Laurent Bopp, C. Anela Choy, Leanne Duffy, Brian Fry, et al.

DR. ANNE LORRAIN (Orcid ID : 0000-0002-1289-2072)

DR. CHRISTOPHER J SOMES (Orcid ID : 0000-0003-2635-7617)

Article type : Primary Research Articles

Title

Trends in tuna carbon isotopes suggest global changes in pelagic phytoplankton communities

Running title

Tuna suggest global phytoplankton changes

Authors

Lorrain[1]*, A., Pethybridge[2], H., Cassar[1,3], N., Receveur[4], A., Allain[4], V., Bodin[5,6], N., Bopp[7], L., Choy[8], C.A., Duffy[9], L., Fry[10], B., Goñi[11], N., Graham[12], BS., Hobday[2], A.J., Logan[13], J.M., Ménard[14], F., Menkes[15] C., Olson[9], D.E., Pagendam[16], R.J., Point[17], D., Revill[2], A.T., Somes[18], C.J., Young[2] J.W.

[1]IRD, Univ Brest, CNRS, Ifremer, LEMAR, F-29280 Plouzané, France.

[2]CSIRO Oceans and Atmosphere, Hobart, Tasmania, Australia

[3]Division of Earth and Ocean Sciences, Nicholas School of the Environment, Duke University, Durham, NC 27708, USA

[4]Pacific Community, Oceanic Fisheries Programme, BP D5, 98848 Nouméa, New Caledonia

[5]IRD, Fishing Port, Victoria, Mahe, Republic of Seychelles

[6]Seychelles Fishing Authority (SFA), Fishing Port, Victoria, Mahe, Republic of Seychelles

[7]Laboratoire de Météorologie Dynamique (LMD), Institut Pierre-Simon Laplace (IPSL), Paris, France

[8]Integrative Oceanography Division, Scripps, Institution of Oceanography, University of California, San Diego, La Jolla, California

[9]Inter-American Tropical Tuna Commission, (IATTC), 8901 La Jolla Shores Dr., La Jolla, CA 92037-1509, USA

[10]Australian Rivers Institute, Griffith, University, Nathan, Queensland, Australia

[11]AZTI, Marine Research, 20110 Pasaia, Gipuzkoa, Spain

[12]National Institute of Water and Atmospheric Research, Ltd. (NIWA), 301 Evans Bay Parade, Greta Point, Wellington 6021, New Zealand

[13]Massachusetts Division of Marine Fisheries, New Bedford, Massachusetts 02744, USA

[14]Aix Marseille Univ., Univ. Toulon, CNRS, IRD, MIO, UM110, Marseille, France

[15]IRD / UMR ENTROPIE, BP A5, 98848 Nouméa cedex, New Caledonia

[16]CSIRO, Computational Informatics, Brisbane, Australia

[17]Observatoire Midi-Pyrénées, GET, UMR CNRS 5563 / IRD 234 / Université Paul Sabatier Toulouse 3, Toulouse, France

[18]GEOMAR Helmholtz Centre for Ocean, Research Kiel, Düsternbrooker Weg 20, 24105 Kiel, Germany

Corresponding author

Anne Lorrain (Tel: +33 2 90 91 55 75, anne.lorrain@ird.fr)

Abstract

Considerable uncertainty remains into how increasing atmospheric CO_2 and anthropogenic climate changes are affecting open-ocean marine ecosystems from phytoplankton to top predators. Biological time series data are thus urgently needed for the world's oceans. Here, we use the carbon stable isotope composition of tuna to provide a first insight into the existence of global trends in complex ecosystem dynamics and changes in the oceanic carbon cycle. From 2000 to 2015, considerable declines in $\delta^{13}C$ values of 0.8 to 2.5‰ were observed across three tuna species sampled globally, with more substantial changes in the Pacific Ocean compared to the Atlantic and Indian Oceans. Tunas not only recorded the Suess effect, i.e. fossil fuel-derived and isotopically-light carbon being incorporated into marine ecosystems, but also profound changes at the base of marine food webs. We suggest a global shift in phytoplankton community structure, e.g. a reduction of ^{13}C-rich phytoplankton such as diatoms, and/or a change in phytoplankton physiology during this period, while this does not prevent other concomitant changes at higher levels in the food webs. Our study establishes tuna $\delta^{13}C$ values as a candidate essential ocean variable to assess complex ecosystem responses to climate change at regional to global scales and over decadal timescales. Finally, this time-series will be invaluable in calibrating and validating global earth system models to project changes in marine biota.

Keywords*: Suess effect, phytoplankton, yellowfin tuna, albacore tuna, bigeye tuna, Pacific Ocean, Indian Ocean, Atlantic Ocean, carbon cycle, biogeochemical cycles*

1. Introduction

Over the past 50 years, 90% of the heat associated with global warming, and 30% of the fossil-fuel carbon emissions have been absorbed by the oceans[1]. Such processes are predicted to severely impact marine biota[2], through enhanced ocean stratification and acidification. Unfortunately, there are large uncertainties on how oceanic ecosystems have changed or may change in the future. For example, the current generation of earth system models simulates a wide range of future changes in global ocean net primary productivity (NPP), with both increases and decreases of up to 20% by 2100[3,4], highlighting large discrepancies in the trends of simulated NPP. Only a limited number of empirical datasets record trends in the phytoplankton community composition or physiology[5–7]. The magnification of relative changes in phytoplankton dynamics across trophic levels has rarely been investigated with few available empirical methods capable of quantifying ecosystem level responses. Biological time-series datasets are imperative for understanding past responses of the world's oceans and for quantifying uncertainty in future climate projections[8].

Carbon stable isotopes ($\delta^{13}C$ values or $^{13}C/^{12}C$) have been used to reconstruct the oceanic carbon cycle using direct measurements or marine archives (e.g., marine sediments, corals) from paleoclimates to the current anthropogenic perturbation[9–12]. Since the Industrial Revolution, the rise in atmospheric CO_2 has been accompanied by a decrease in the carbon isotope ratio of atmospheric CO_2, known as the Suess effect[13]. This decrease is attributed to the atmospheric release of isotopically-light carbon from fossil fuel combustion. Due to the oceanic uptake of this ^{13}C-depleted CO_2, the oceanic $\delta^{13}C$ value of dissolved inorganic carbon ($\delta^{13}C_{DIC}$) is decreasing[14,15]. Changes in $\delta^{13}C_{DIC}$ values are recorded in phytoplankton $\delta^{13}C$ values after accounting for an isotopic fractionation factor associated with photosynthesis (defined as ε_p). Isotopic fractionation is dependent on seawater characteristics, phytoplankton composition and physiology. The primary factors that are believed to affect the isotopic values of phytoplankton are: 1) the concentration and $\delta^{13}C$ values of dissolved CO_2 ([CO2]aq)[16–18]), 2) phytoplankton community composition and cell morphology[18], and 3) cellular growth rate[17,19]. Secondary physiological traits (e.g., decreases in bicarbonate uptake or in carbon-concentrating mechanism activity) can also impact isotopic values, but are difficult to model[20].

Carbon isotopic changes at the base of food webs are transferred to higher trophic levels with values increasing slightly (typically 0.5 to 1‰) with each trophic transfer[21,22]. Metabolically active tissues of consumers (e.g., fish muscle) integrate the stable isotope values of this base through

their diet[22,23]. While nitrogen isotope ($\delta^{15}N$) values are commonly used to investigate changes in trophic levels, $\delta^{13}C$ values provide information on animal diets and on spatial variations at the base of food webs[23–25]. Historical studies focusing on baseline changes have examined accretionary bioarchives that suffer little degradation after formation such as keratin baleen plates, feathers or teeth dentin of marine consumers that reflect the food they ingest and therefore, the $\delta^{13}C$ values of phytoplankton[26–28]. These studies demonstrate the utility of isotope measurements to reconstruct past and present ocean primary productivity, and provide evidence of past climate changes at regional scales[27–29]. Finally, metabolically-inert but inorganic accretionary structures (e.g., bivalve shells, coral skeleton, sclerosponges or fish otoliths) can also reflect the $\delta^{13}C_{DIC}$ value of the environment across their lifetime[30,31] as they usually precipitate in equilibrium with seawater, although vital effects can complicate environmental reconstruction[32,33]. Similarly, $\delta^{13}C$ values of metabolically active tissues may reflect trends in physio-chemical processes (CO_2 and $\delta^{13}C_{aq}$ values) and biological processes (phytoplankton $\delta^{13}C$ values).

The aim of our study was to assess trends in a time-series of stable isotope values of metabolically active tuna tissues, and to test if this could be used to detect ecosystem level responses over decadal time scales at regional to global scales. For this purpose, we analyzed $\delta^{13}C$ and $\delta^{15}N$ values of muscle samples from three species of tuna (yellowfin tuna, *Thunnus albacares*; bigeye tuna, *T. obesus*; and albacore tuna, *T. alalunga*) collected throughout tropical, sub-tropical, and temperate oceans from 2000 to 2015 (n=4,477; Fig. 1). Each of these species has different vertical and foraging distributions (from surface to mesopelagic depths[34]). Therefore, our study seeks to resolve broad horizontal and vertical spatial patterns in oceanic food webs. As tuna are widely distributed and harvested globally[35], they are good candidates to study how observed and suspected changes in physical and biological processes at global and ocean basin scales may be reflected in consumer $\delta^{13}C$ values. We developed a theoretical model to decompose the observed temporal changes in consumer $\delta^{13}C$ values into putative causal contributors. The model accounted for (1) known temporal trends in fossil fuel-derived carbon (the Suess effect) and CO_2 availability, (2) possible changes in phytoplankton dynamics including community composition and growth rates and (3) potential changes in trophic fractionation factor. Our study, which focuses on carbon but draws on nitrogen isotopes to assess potential changes in tuna trophic positions, suggests large-scale shifts in phytoplankton communities from 2000 to 2015.

2. Materials and Methods

Tuna carbon isotope data

We assembled a global database using published and unpublished regional carbon isotope studies resulting in 4,477 records from 2000 to 2015. Details on isotopic methods and predator sampling are provided in Pethybridge et al.[36] that analyzed the same global dataset but for $\delta^{15}N$ values. As for $\delta^{15}N$ and other global compilation studies[37], we assumed that the agreement between $\delta^{13}C$ values generated across different laboratories was < 0.2-0.3‰. Tuna size (fork length, in cm) was measured for each individual. Tuna were sampled from three ocean basins (Atlantic, Indian and Pacific Ocean) with albacore tuna occupying more temperate waters compared to the tropical yellowfin and bigeye tunas (Fig. 1,[34]).

The Pacific Ocean had the most extensive sampling with 2,504 individuals and no gap from 2000 to 2015, except for albacore where data was not available for 4 years. In the Indian and Atlantic Oceans, data were more scattered (Table S1). Pelagic tuna are mobile predators and the stable carbon isotopic composition of their muscle tissue represents an integration of their foraging environment over approximately 6 months to one year[38]. Tuna muscle tissue $\delta^{13}C$ values were corrected for lipids in all samples either with chemical extraction or using a mass balance equation for elevated lipid content samples (C/N>3.5) with parameters derived from Atlantic bluefin tuna (*T. thynnus*) muscle[39].

Temporal trends in tuna $\delta^{13}C$ values

Time series analyses based on multiple linear regression analysis, performed using the R-3.2.4 software[40] and the nlme package[41] were used to examine and test for significant linear trends in tuna carbon isotope values. To ensure that tuna length (size) did not have any effect on potential temporal trends, an interaction between size and year was tested and was not found to be significant for the Pacific or Atlantic Oceans. For the global dataset, we tested a model with tuna size included, by species and ocean basins, and then fitted a model explaining the residuals of this first model as a function of year. The slopes were similar to those obtained without the effect of size included, meaning that the addition of size does not change the observed patterns and that this factor has a small impact on temporal trends in $\delta^{13}C$ values. We finally tested for three variables: year (quantitative), ocean with three levels (Atlantic, Indian and Pacific Ocean), and tuna species with three levels (albacore, bigeye and yellowfin). All combinations were tested and the final

model was chosen using the AIC (Akaike information criterion). We added an auto-correlation structure: a one-degree ARIMA[41] via the gls function (autoregressive integrated moving average) fitted by groups of tuna sampled at the same date and position. Auto-correlation structures on residuals were checked with an ACF (auto correlation function). Finally, to account for possible spatial biases (i) in years of sampling according to locations (Fig. S1) or (ii) due to baseline isotopic variations across space[42], tuna $\delta^{13}C$ trends were also determined at a smaller spatial scale by considering one region where sufficient data were available per year, i.e., New Caledonia and Fiji (see Fig. 1 for selected region area) and with similar isotope values at the base of the food web[38,43]. Furthermore, all New Caledonia and Fiji samples were analysed in the same laboratory and time period.

Modeling the factors influencing tuna $\delta^{13}C$ values

We developed a theoretical model to explain the potential effects of various factors and processes known to explain trends in tuna $\delta^{13}C$ values. First, we considered the isotope value of phytoplankton ($\delta^{13}C_p$) that has been shown to be driven by the magnitude of carbon isotopic fractionation during photosynthesis (ε_p) and the isotope value of CO_2 ($\delta^{13}C_{aq}$, i.e., Suess effect), with ε_p dependent on the carbon isotope fractionation associated with carbon fixation (ε_f) and the specific growth rate (μ)[16].

$$\delta^{13}C_p = \frac{1}{\left(1 + \frac{\varepsilon_p}{1000}\right)}(\delta^{13}C_{aq} - \varepsilon_p) \quad \text{Eq. 1}$$

with

$$\varepsilon_p = \varepsilon_f - \frac{b\mu}{CO_2} \quad \text{Eq. 2}$$

where 'b' is a constant ($mM.d^{-1}$) reflecting the degree of dependence of fractionation on the CO_2 concentration, and is believed to vary between species and as a function of growth conditions[19,44]. While the parameter values are arbitrary, they are within the range of values reported in the literature (Table 1). An initial value of 120 was used for b which is consistent with the range of values (52.6 to 137.9) from Popp et al.[18] for *Emiliana huxleyi* ($\varepsilon_p = 24.6 - 137.9\mu/CO_2$) the most common species of coccolithophore globally[45], and *Phaeodactylum tricornutum* (ε_p = 25.5 -

52.6μ/CO_2), a diatom mostly used in laboratory studies but not representative of the global ocean. For the intrinsic fractionation during photosynthesis by the enzyme Rubisco (ε_f), we used a value of 25‰ for ε_f, which has been estimated to range between ~ 22 and 30‰ depending on species (e.g.,[18]), with values as low as 11‰ for the Rubisco of the coccolithophore *Emiliania huxleyi*[46]. The value of 25‰ for ε_f has often been proposed[19] in studies trying to understand temporal trends in marine chronologies[28]

While precise estimates of ε_f or b are not available, this parametrization provides a quantitative demonstration of how even small changes in phytoplankton community composition or physiology may influence tuna muscle $\delta^{13}C$ values, and hence emergent signals of change (Table 1). Growth rate μ was set at 0.3 d^{-1} as it is the median value at Station Aloha[47] in the central North Pacific (Hawaii Ocean Time-series, HOTS) and was also used by several authors[44]. Ranges for μ from 0.1 to 1 d^{-1} have been reported in the literature[47,48]. We proposed a decrease of growth rate of up to 15% over the 2000-2015 study period (from 0.30 to 0.26), which is on the high-end of observed modern changes[5] and predicted decreases for the future[4]. The $\delta^{13}C_{aq}$ values were taken from Station ALOHA[15].

Changes in tuna $\delta^{13}C$ values can in turn be described by the following equation:

$$\delta^{13}C_{tuna} = \frac{1}{\left(1 + \frac{\varepsilon_{fc}}{1000}\right)}\left(\delta^{13}C_p - \varepsilon_{fc}\right) \quad \text{Eq. 3}$$

where ε_{fc} is the overall fractionation associated with trophic transfers and is considered to be low (~0.5 to 1.8‰ per trophic level, therefore we used 4‰ for tuna that are considered to be at a trophic position of ~4, [34]). As a comparison, Bird et al.[37] found an average difference of 4.6‰ between phytoplankton and sharks on a global scale.

Combining Eq. 2 with Eq. 3 leads to:

$$\delta^{13}C_{tuna} = \frac{1}{\left(1+\frac{\varepsilon_{fc}}{1000}\right)}\left(\left(\frac{1}{\left(1+\frac{\left(\varepsilon_f-\frac{b\mu}{CO_2}\right)}{1000}\right)}\left(\delta^{13}C_{aq}-\left(\varepsilon_f-\frac{b\mu}{CO_2}\right)\right)\right)-\varepsilon_{fc}\right)$$

Eq. 4

We used two different parametrizations developed in the literature on the effect of the concentration of CO_{2aq} on the isotope values of phytoplankton[19,20]. Indeed, while the first parametrization[16,19] provides quantitative intuition for the dependence of tuna $\delta^{13}C$ values on phytoplankton physiology, it does not account for additional factors influencing the phytoplankton isotope values, including changes in the carbon source (bicarbonate vs. CO_2), deactivation of carbon-concentrating mechanisms in response to increased CO_2 availability, and changes in the growth conditions (nutrient vs. light limitation). For completeness, we also show the predictions based on the parametrization presented in Cassar et al.[20]. The sensitivity of tuna $\delta^{13}C$ values to each factor was assessed by calculating the ratio of the percentage change of tuna $\delta^{13}C$ values to percentage change of each factor. The slope ('m') of each curve is related to the ratio of the percentage change of tuna $\delta^{13}C$ values to percentage change of each factor according to the following equation:

$$\left(\frac{d\delta^{13}C_{tuna}}{\delta^{13}C_{tuna}}\right)\left(\frac{dx}{x}\right) = m.\frac{x}{\delta^{13}C_{tuna}}$$

Eq. 5

This sensitivity analysis examines the influence of one parameter at a time on tuna isotopic composition with assumed initial values for each parameter based on literature. To reinforce this analysis, we conducted a Bayesian approach that takes into account the uncertainty of all parameters simultaneously to explain tuna isotopic composition with ranges and uncertainties taken from literature values (Supplementary Analysis 1). To reconstruct the observed trends in tuna $\delta^{13}C$ values, a number of scenarios were run to simulate percentage changes in the phytoplankton parameters μ, b and ε_f or ε_{fc} (Table 1). These scenarios were used to resolve competing hypotheses for the observed patterns.

3. Results

Trends in $\delta^{13}C$ values

Over the entire record (Fig. 1), individual tuna $\delta^{13}C$ values ranged from -19.9 to -12.9‰. Mean annual $\delta^{13}C$ values decreased by 0.8 to 2.5‰ within species and ocean basins from 2000 to 2015 (Table 2, Fig. 2). These negative trends were significant, with similar observed slopes for each tuna species by ocean basin ($p < 0.0001$; Table 2). The largest decrease was observed for the Pacific Ocean and the lowest in the Indian Ocean, with the Atlantic Ocean intermediate. For reference, we showed a global decreasing trend acknowledging that most of our observations were from the Pacific (56%) (Table 2, Fig. 2, 1.8‰ decrease from 2000 to 2015), while observations from the Indian and Atlantic Ocean each comprised 22% of the data (Table 2).

In the region of New Caledonia and Fiji, where we have the most complete record to derive a temporal trend (Supplementary Fig. S1), the same decreasing pattern in tuna $\delta^{13}C$ values was observed for all three species (2.1‰ decrease between 2000 and 2015, Supplementary Fig. S2) as over the broader Pacific region (2.5‰ decrease). No temporal changes in $\delta^{15}N$ values were observed for the three tuna species in the New Caledonia and Fiji regions (Supplementary Fig. S3), suggesting no significant tuna trophic position changes over the record. Some weak trends in $\delta^{15}N$ values were found for some species and ocean basins, which could arise from the interaction with other confounding factors such as tuna size and location (Supplementary Fig. S4). Two likely explanations for the observed tuna $\delta^{13}C$ trends are discussed below.

Accounting for the observed Suess effect and CO_2 availability

Reported declines in $\delta^{13}C_{aq}$ values at Station ALOHA during the 2000-2015 period (-0.3‰) explained 14% of the decrease in tuna $\Delta\delta^{13}C$ values observed in our New Caledonia-Fiji region (Fig. 3a).

Assuming similar Suess effects in the other ocean basins, 12%, 22% and 38% of the decrease in tuna $\delta^{13}C$ values in the Pacific, Atlantic and Indian Oceans, respectively can be explained by $\delta^{13}C_{aq}$ (Table 1).

An increase in the concentration of CO_{2aq} observed at Station ALOHA also leads to a decrease in tuna $\delta^{13}C$ values by increasing carbon isotopic fractionation during photosynthesis ε_p (Eq. 2).

Depending on the parametrization used to account for this effect[19,20], 2 to 35% of the trend in tuna $\delta^{13}C$ values can be explained by changes in CO_2 availability in the New Caledonia-Fiji region (Fig. 3b). Using the larger degree of change in response to CO_2 availability[19], percentages of change similar to those from the Suess effect can be explained across the different ocean basins. The additive impacts of CO_2 availability and the Suess effect in explaining tuna $\Delta\delta^{13}C$ values are 23%, 41%, and 73% in the Pacific, Atlantic and Indian Oceans, respectively. If the CO_2 availability effect reported by Cassar et al.[20] is used, in addition to the Suess effect, then only 14%, 26% and 46% of the $\Delta\delta^{13}C$ decrease in the Pacific, Atlantic and Indian Oceans can be explained.

Hypothesized changes in phytoplankton dynamics

According to theoretical models (see method section), the then unexplained temporal changes in tuna $\delta^{13}C$ values (~27-86%) must be related to a (i) decrease in phytoplankton cellular growth rates (μ) or physiology (e.g., carbon-concentrating mechanism activity), and/or (ii) potential changes in phytoplankton communities (through changes in species dependent parameters b and ε_f) or in the trophic fractionation factor ε_{fc}. Based both on the sensitivity analysis and the Bayesian inference, variations in growth rate μ and trophic fractionation factor (ε_{fc}) have a small effect on tuna isotope values (Table 1 and Supplementary Analysis 1). As an example, an imposed substantial 15% decrease in the growth rate μ over 16 years resulted in only a 0.48‰ decrease in tuna $\delta^{13}C$ values (Fig. 3c, around 20% of the total decrease in the New Caledonia-Fiji region and in the broader Pacific Ocean). This effect is larger in the Atlantic (35%) and Indian (62%) Oceans. However, more reasonable declines of 5 and 10% of μ over 16 years resulted in smaller decreases of 0.2‰ and 0.3‰ in tuna $\delta^{13}C$ values from 2000 to 2015, respectively (Table 1), which explained 8 to 38% of this overall signal in various ocean basins. Variations in the trophic fractionation factor ε_{fc} were of similar order (Table 1) with large decreases of this parameter needed to explain the tuna $\delta^{13}C$ pattern.

The carbon fixation fractionation factor (ε_f) and 'b' values can vary widely among phytoplankton species[18]. The sensitivity analysis and the Bayesian model (that takes into account a large range of values for these parameters) showed that the carbon fixation fractionation factor ε_f had the largest effect on the tuna isotope values compared to all other factors (Table 1 and Supplementary Analysis 1). As an example, we arbitrarily set the changes to 5% for ε_f and 10% for b (Fig. 3d) to

reflect their differential impact on tuna $\Delta\delta^{13}C$ values. This small 5% increase in ε_f resulted in a large decrease in tuna carbon isotope values of 1.2‰ (i.e., ~ 50% of the tuna $\Delta\delta^{13}C$ in the New Caledonia-Fiji region and the Pacific Oceans (Fig. 3d, Table 1)). In comparison, a 10% decline in 'b' values only causesd a 0.5‰ decline in tuna $\delta^{13}C$ values, which explained 20-36% in the Pacific and Atlantic Ocean, and 64% in the Indian Ocean.

After accounting for the Suess and CO_2 availability effects, several permutations for the parameters reflecting productivity (μ) and species composition (with changes in ε_f and *b* combined) may account for the remaining $\Delta\delta^{13}C$ changes. The combination of the Suess effect, the effect of increasing $[CO_2]_{aq}$ concentrations on ε_p, and a change of 5 to 10% in species-specific parameters (10% for b and 5% for ε_f) with no change in productivity or trophic fractionation factor ε_{fc}, produced a 2.1‰ decrease in tuna $\delta^{13}C$ values, consistent with the observed change in the Pacific Ocean (Fig. 3d). In the Pacific Ocean, where we have the most robust dataset, changes in phytoplankton parameters seem to have occurred, unless we assume that growth rates have changed by > 70%. If we assume that no changes in growth rates and ε_{fc} have occurred and use the Bidigare et al.[19] parametrization, then more than 60% of $\Delta\delta^{13}C$ has to be explained by a change in species composition in the Pacific and Atlantic Ocean, against only 27% in the Indian Ocean (Table 1). The use of the Cassar et al.[20] parametrization implies even larger changes in species composition. Averaging all tuna species and all ocean basins, and both parametrizations used to calculate carbon fractionation from phytoplankton, the global trend in tuna $\delta^{13}C$ values ($\Delta\delta^{13}C$) can for example be explained by (i) the observed Suess effect and increases in CO_{2aq} (up to 26%), (ii) a 5 % decrease in productivity (11%), a 10% decrease in trophic fractionation factor (17%) and (iv) imposed changes of 5% in species-specific parameters indicating a shift in species composition (46%) (Fig. 4). While this is one potential scenario, in part informed and constrained by observations in the literature[5,6], there are a multitude of permutations that may fit the observed trend. Nevertheless, changes in species dependent parameters (ε_f) had the largest effects in the simulations using both modelling approaches, and better accounted for the observed tuna trends than changes in productivity, trophic fractionation factor (ε_{fc}) or even the known Suess effect.

4. Discussion

Our analysis revealed that changes in the biological component of the marine carbon cycle can be traced in the tissues of marine top predators. We observed substantial and widespread declines in tuna muscle $\delta^{13}C$ values (by 0.8 to 2.5‰) in three tuna species across three ocean basins. Such a trend over a 16-year period has never been recorded in metabolic tissues of a marine predator. The use of two separate modelling approaches (sensitivity analysis and Bayesian inference) revealed that the parameter linked to phytoplankton fractionation (ε_f) had the largest influence on the observed temporal trend in tuna muscle $\delta^{13}C$ values. Our calculations then suggest that up to 60% of the decrease in tuna $\delta^{13}C$ values seems to be due to a change in phytoplankton parameters in the Pacific Ocean, compared to only 27% in the western Indian Ocean. While our most robust dataset is from the Pacific Ocean, the same decreasing pattern in tuna $\delta^{13}C$ values in all ocean basins (Pacific, Atlantic and western Indian) suggests a widespread shift in marine plankton communities or a change in their physiology, but does not exclude other factors that may act in synergy (e.g., a change of productivity or trophic fractionation factor).

Previously reported temporal changes in $\delta^{13}C$ values are generally attributed to the Suess effect or changes in marine productivity in various organisms and ecosystems[27,28,30]. For example, Schell[28] found a significant long-term decline in $\delta^{13}C$ values in inert baleen plates (~2.7‰) over a 30-year period (between 1965 and 1997) attributing this decline to a ~30 to 40% decline in primary productivity in the Bering Sea. Cullen et al.[44] proposed that part of the decrease observed by Schell[28] was due to the Suess effect and to the influence of changes in CO_2 concentration on phytoplankton physiology (as shown in Fig. 3b and described herein). In contrast, the Suess effect is relatively small over our time period (0.3‰, Fig. 3a) and only explains ~12-20% of the observed decrease in tuna muscle $\delta^{13}C$ values (in the Atlantic and Pacific Oceans). Similarly, increasing CO_2 concentrations only explain a small percentage (~2-18%, Table 1) of the observed decrease in muscle tuna $\delta^{13}C$ values, using the Bidigare et al.[19] or Cassar et al.[20] parametrizations for their effect on the carbon fixation factor fractionation.

After accounting for the observed Suess effect and changes in $[CO_2]_{aq}$ availability, our model was used to explore how changes in phytoplankton growth rates and species composition can further reconstruct our observed declines in tuna muscle $\delta^{13}C$ values. The sensitivity, Bayesian and scenario analysis demonstrated that relatively small changes in phytoplankton community composition can lead to large declines in tuna $\delta^{13}C$ values (Table 1 and Supplementary Analysis 1), while larger changes in productivity or trophic fractionation factor would be needed. In our

study, a 15% decrease in phytoplankton productivity cannot explain the decline we observed in tuna muscle $\delta^{13}C$ values, even when combined with the Suess effect and the cumulative effect of increasing $[CO_2]_{aq}$ concentrations on ε_p. The change in productivity that we tested in this study is at the higher end of previously reported declines (typically ranging between 0-1.4% yr^{-1} at the regional to ocean basin scale[7,49,50]). Other studies have shown no recent trends in global primary productivity[5,51] and some regional increases have been reported historically (e.g. Pacific Ocean[52]). Even in model studies, projections of global marine net primary productivity are highly uncertain with relative changes between -20 and +20% over the 21st century[4].

The rate of decrease observed in our tuna $\delta^{13}C$ values requires concomitant changes in phytoplankton parameters (εf and b). Young et al.[53] already reported evidence of change in the biological carbon isotopic fractionation by phytoplankton (ε_p) with significant increases between 1960 and 2010, in particular in the subtropics, where this change was the highest compared to other regions. The change in biological fractionation estimated through their model (i.e., a maximum of 0.4‰ in 16 years) is 2 to 5 five times lower than our observations in tuna, depending on the ocean basin. Their study is based on a compilation of POC data from several transects mostly from the Atlantic Ocean with few data in our Pacific region, which could explain the differences between their model and our observations. However, they showed a time series of $\delta^{13}C$ particulate organic carbon (δ^{13}_{POC}) values in the North Atlantic off Bermuda with a 2‰ decrease from 1980 to 2007 (i.e., ~ 1.2‰ decrease in 16 years). This result is similar to the 1.4‰ decrease in tuna values we observed in the Atlantic from 2000 to 2015.

Support for our hypothesis of a shift in marine plankton communities already exists[6,54–56]. Diatoms are predicted to decrease in abundance in response to increased seawater stratification with a reported decline of 1.22% yr^{-1} in the North Pacific[6]. Such a reduction in the abundance of diatoms, a ^{13}C-rich carbon source in marine food webs[57], is expected to decrease the $\delta^{13}C$ values of consumers, and this diatom contribution has been emphasized in a recent model of phytoplankton $\delta^{13}C$ variations in the global ocean[43]. Tuerana et al.[58] also recently found that cell size was the primary determinant of δ^{13}_{POC} in the South Atlantic subtropical convergence zone and predicted that isotopic carbon fractionation will increase in the future, leading to lower δ^{13}_{POC} that may

propagate through the food web. A decrease in the abundance of coccolithophores, another ^{13}C-rich carbon source, might also explain some of the tuna $\delta^{13}C$ trend. However, Rivero-Calle et al.[59] found an increase in the occurrence of coccolithophores in the North Atlantic, but data are not available at a global scale. Ocean basin differences found in our study in the temporal slopes in tuna $\delta^{13}C$ values between the Indian Ocean (0.8‰) and the Atlantic and Pacific Oceans (from 1.4 to 2.5‰) could be due to a combination of several factors. The magnitude of the Suess effect may vary regionally[15]. Changes in phytoplankton communities or physiology are also dependent on regional-scale processes[60,61]. The use of spatially resolved models of the ocean ^{13}C cycle would help to understand the regional differences[62].

5. Caveats and limitations

Phytoplankton have many strategies to take up carbon as a function of growth conditions that could affect fractionation. For example, a decrease in bicarbonate uptake or carbon-concentrating mechanism activity in general would be predicted to increase the apparent fractionation. Our predictions should therefore be interpreted with caution as isotopic fractionation is not a single function of μ/CO_2, even within a single phytoplankton species[20,63]. Furthermore, other permutations of ε_f or b may fit the observed decrease. However, this parametrization together with the Bayesian inference demonstrates how small changes in phytoplankton community composition or physiology may influence tuna muscle $\delta^{13}C$ values.

We also note that regional variations cannot be captured by the time series of $\delta^{13}C_{aq}$ at Station Aloha (Hawaii, Pacific). Long-term declines of $\delta^{13}C_{aq}$ values due to the combination of the Suess effect, vertical mixing and primary production (residual carbon pool after particulate organic carbon production) have been documented at other monitoring stations, with varying effects according to region and latitude, in particular in the southern regions[64]. However, both instrumental and proxy records of $\delta^{13}C_{aq}$ indicate a consistent average decrease per year of 0.027‰ at 5 Pacific stations from Hawaii to American Samoa since 1980 (corresponding to an approximately 0.4‰ decline in our 16 year period[12]). Furthermore, Gruber et al.[65] compared the $\delta^{13}C_{aq}$ trends in several oceanic regions and found that the highest decrease of 0.025‰ was in the subtropical gyres (Bermuda and Hawaii) and the lowest in the equatorial upwelling region of the

Pacific (0.015‰), with the Indian Ocean displaying a decrease of 0.020‰ per year. Therefore, the predicted ranges in all oceanic regions of 0.2 to 0.4‰ decrease over our study period of 16 years, is too small to explain the 1.8‰ average decline in tuna $\delta^{13}C$ values.

Other factors, related to food web or dietary processes, could also influence the tuna $\delta^{13}C$ trend. Size differences in sampled tuna through time could introduce a bias but no consistent relationship between tuna size and $\delta^{13}C$ and $\delta^{15}N$ values or any size changes with time among tuna species were observed (Fig. S5 and S6). While decadal shifts in the diet of yellowfin tuna have been recorded in the eastern Pacific Ocean from the 1990s to the 2000s[66], the similar $\delta^{13}C$ slopes observed for the three tuna species in our study seem inconsistent with changes in foraging location or diet. A shift in the tuna foraging range or timing could also be argued to explain the observed decrease in tuna $\delta^{13}C$ values as there are large spatial and intra-annual variability in the $\delta^{13}C$ values of phytoplankton[43]. Similarly, if all tuna foraged deeper on more mesopelagic prey that had lower $\delta^{13}C$ values than surface prey ($\delta^{13}C_{DIC}$ is known to decrease with depth[67]), tuna $\delta^{13}C$ values would decrease. However, the slope of this decrease would vary among species given that yellowfin tuna mainly inhabit surface waters while bigeye tuna mostly forage in mesopelagic waters[34]. A decrease in the trophic fractionation factor ε_{fc} would reduce tuna $\delta^{13}C$ values through time (Table 1, Figure 4). Various processes including a change in food chain length, food web structure, quality of food or tuna metabolism[68] could alter ε_{fc}. A change in the overall trophic fractionation factor could therefore occur at multiple levels of the food web, driven or not by changes at the base of the food web. As far as we know, there are no data available in the literature to explore this further. However, while we cannot however rule out the possibility that changes in food web structure are negated by changes in source ^{15}N (e.g. denitrification vs. N_2 fixation,[69,70]), we did not see temporal changes in tuna $\delta^{15}N$ values at global or ocean basin scales, suggesting little change in food chain length or structure.

Finally, our dataset has some limitations inherent to the sampling and we acknowledge that our most robust analysis is for the Pacific Ocean that covers a large area with many individuals by year and species (Table S1). More data over broad reaches of the Atlantic and Indian Oceans are needed to provide robust estimates of biological changes in these oceans

6. Concluding remarks

We showed that $\delta^{13}C$ values of metabolically active tissues of mobile marine predators likely reflect recent changes at the base of marine food webs. We detected a substantial worldwide decrease in tuna $\delta^{13}C$ values over the 2000-2015 period which can be related to various processes known to influence ocean carbon cycling in the global oceans. Our analysis suggests that phytoplankton species (e.g., diatoms) that undergo a larger fractionation of carbon during photosynthesis (and thus have higher $\delta^{13}C$ values) have been decreasing over recent decades or that these phytoplankton communities altered their physiologies. While we cannot rule out a widespread decline in phytoplankton productivity, we showed that even a large (>15%) decline would have a small impact on tuna $\delta^{13}C$ values and cannot fully explain the observed global trend. While recognising that a concomitant shift at higher levels of food webs (change in the trophic fractionation factor or in tuna diet or physiology) could occur and that more tuna carbon isotope data are needed from the Atlantic and Indian Oceans, the present study expands our understanding of the main factors that affect the isotopic values of top predators and provides a framework to interpret and model carbon cycling at regional to global scales. New observational or modelled data that provide estimates of periodic changes in marine plankton communities will enable our model to provide estimates of the other contributing factors. Finally, the framework presented here, through the study of tuna carbon and nitrogen isotopes values, could support development of a useful essential ocean variable (EOV) for implementation within a global ocean observing system to document complex ecosystem changes at regional to global scales and over relatively short timescales (decades to centuries). The use of predator isotopes as an EOV would complement regional efforts to acquire *in situ* measurements of plankton abundance and diversity[71].

7. Acknowledgments

We thank the observer programs and the many observers and researchers who collected the samples in each of the ocean basins. This work contributes to CLIOTOP WG3-Task team 01. N.C. was supported by the "Laboratoire d'Excellence" LabexMER (ANR-10-LABX-19) and co-funded by a grant from the French government under the program "Investissements d'Avenir". We thank P. Quay who kindly provided data from Station ALOHA, E.A. Laws for helpful discussions on the manuscript and the three reviewers for their thorough reviews.

8. References

1. Le Quere, C. *et al.* Global carbon budget 2017. *Earth Syst. Sci. Data* **10**, 405–448 (2018).
2. Poloczanska, E. S. *et al.* Responses of marine organisms to climate change across Oceans. *Front. Mar. Sci.* **3**, (2016).
3. Bopp, L. *et al.* Multiple stressors of ocean ecosystems in the 21st century: Projections with CMIP5 models. *Biogeosciences* **10**, 6225 –6245 (2013).
4. Kwiatkowski, L. *et al.* Emergent constraints on projections of declining primary production in the tropical oceans. *Nat. Clim. Change* **7**, 355–358 (2017).
5. Gregg, W. W., Rousseaux, C. S. & Franz, B. A. Global trends in ocean phytoplankton: a new assessment using revised ocean colour data. *Remote Sens. Lett.* **8**, 1102–1111 (2017).
6. Rousseaux, C. S. & Gregg, W. W. Recent decadal trends in global phytoplankton composition. *Glob. Biogeochem. Cycles* **29**, 2015GB005139 (2015).
7. Gregg, W. W. & Rousseaux, C. S. Decadal trends in global pelagic ocean chlorophyll: A new assessment integrating multiple satellites, in situ data, and models. *J. Geophys. Res. Oceans* **119**, 5921–5933 (2014).
8. Bonan, G. B. & Doney, S. C. Climate, ecosystems, and planetary futures: The challenge to predict life in Earth system models. *Science* **359**, eaam8328 (2018).
9. Freeman, K. H. & Hayes, J. M. Fractionation of carbon isotopes by phytoplankton and estimates of ancient CO_2 levels. *Glob. Biogeochem. Cycles* **6**, 185–198 (1992).
10. Ehleringer, J. R., Buchmann, N. & Flanagan, L. B. Carbon isotope ratios in belowground carbon cycle processes. *Ecol. Appl.* **10**, 412–422 (2000).
11. Keeling, R. F. *et al.* Atmospheric evidence for a global secular increase in carbon isotopic discrimination of land photosynthesis. *Proc. Natl. Acad. Sci.* **114**, 10361–10366 (2017).
12. Wu, H. C. *et al.* Surface ocean pH variations since 1689 CE and recent ocean acidification in the tropical South Pacific. *Nat. Commun.* **9**, 2543 (2018).
13. Keeling, C. D. The Suess effect: ^{13}Carbon-^{14}Carbon interrelations. *Environ. Int.* **2**, 229–300 (1979).

14. Quay, P. *et al.* Anthropogenic CO_2 accumulation rates in the North Atlantic Ocean from changes in the $^{13}C/^{12}C$ of dissolved inorganic carbon. *Glob. Biogeochem. Cycles* **21**, GB1009 (2007).
15. Quay, P., Sonnerup, R., Munro, D. & Sweeney, C. Anthropogenic CO_2 accumulation and uptake rates in the Pacific Ocean based on changes in the $^{13}C/^{12}C$ of dissolved inorganic carbon. *Glob. Biogeochem. Cycles* **31**, 2016GB005460 (2017).
16. Laws, E. A., Popp, B. N., Bidigare, R. R., Kennicutt, M. C. & Macko, S. A. Dependence of phytoplankton carbon isotopic composition on growth rate and $[CO_2]$aq: Theoretical considerations and experimental results. *Geochim. Cosmochim. Acta* **59**, 1131–1138 (1995).
17. Fry, B. $^{13}C/^{12}C$ fractionation by marine diatoms. *Mar. Ecol. Prog. Ser.* **134**, 283–294 (1996).
18. Popp, B. N. *et al.* Effect of phytoplankton cell geometry on carbon isotopic fractionation. *Geochim. Cosmochim. Acta* **62**, 69–77 (1998).
19. Bidigare, R. R. *et al.* Consistent fractionation of ^{13}C in nature and in the laboratory: Growth-rate effects in some haptophyte algae. *Glob. Biogeochem. Cycles* **11**, 279–292 (1997).
20. Cassar, N., Laws, E. A. & Popp, B. N. Carbon isotopic fractionation by the marine diatom *Phaeodactylum tricornutum* under nutrient-and light-limited growth conditions. *Geochim. Cosmochim. Acta* **70**, 5323–5335 (2006).
21. Fry, B. *Stable Isotope Ecology*. (Springer, 2006).
22. Graham, B. S., Koch, P. L., Newsome, S. D., McMahon, K. W. & Aurioles, D. Using isoscapes to trace the movements and foraging behavior of top predators in oceanic ecosystems. in *Isoscapes* (eds. West, J. B., Bowen, G. J., Dawson, T. E. & Tu, K. P.) 299–318 (Springer Netherlands, 2010).
23. Cherel, Y. & Hobson, K. A. Geographical variation in carbon stable isotope signatures of marine predators: a tool to investigate their foraging areas in the Southern Ocean. *Mar. Ecol. Prog. Ser.* **329**, 281–287 (2007).
24. Trueman, C. N., MacKenzie, K. M. & Palmer, M. R. Identifying migrations in marine fishes through stable-isotope analysis. *J. Fish Biol.* **81**, 826–847 (2012).
25. MacKenzie, K. M., Longmore, C., Preece, C., Lucas, C. H. & Trueman, C. N. Testing the long-term stability of marine isoscapes in shelf seas using jellyfish tissues. *Biogeochemistry* **121**, 441–454 (2014).

26. Jaeger, A. & Cherel, Y. Isotopic investigation of contemporary and historic changes in penguin trophic niches and carrying capacity of the Southern Indian Ocean. *PLOS ONE* **6**, e16484 (2011).
27. Newsome, S. D. *et al.* Historic decline in primary productivity in western Gulf of Alaska and eastern Bering Sea: isotopic analysis of northern fur seal teeth. *Mar. Ecol. Prog. Ser.* **332**, 211–224 (2007).
28. Schell, D. M. Carbon isotope ratio variations in Bering Sea biota: The role of anthropogenic carbon dioxide. *Limnol. Oceanogr.* **46**, 999–1000 (2001).
29. Hobson, K. A., Sinclair, E. H., York, A. E., Thomason, J. R. & Merrick, R. E. Retrospective isotopic analyses of steller zea lion tooth annuli and seabird feathers: a cross-taxa approach to investigating regime and dietary shifts in the Gulf of Alaska. *Mar. Mammal Sci.* **20**, 621–638 (2004).
30. Fraile, I. *et al.* The imprint of anthropogenic CO_2 emissions on Atlantic bluefin tuna otoliths. *J. Mar. Syst.* **158**, 26–33 (2016).
31. Swart, P. K. *et al.* The^{13}C Suess effect in scleractinian corals mirror changes in the anthropogenic CO_2inventory of the surface oceans. *Geophys. Res. Lett.* **37**, L05604 (2010).
32. Lorrain, A. *et al.* δ^{13}C variation in scallop shells: Increasing metabolic carbon contribution with body size? *Geochim. Cosmochim. Acta* **68**, 3509–3519 (2004).
33. McConnaughey, T. A. & Gillikin, D. P. Carbon isotopes in mollusk shell carbonates. *Geo-Mar. Lett.* **28**, 287–299 (2008).
34. Olson, R. J. *et al.* Chapter Four - Bioenergetics, trophic ecology, and niche separation of tunas. In *Advances in Marine Biology* (ed. Curry, B. E.) **74**, 199–344 (Academic Press, 2016).
35. Majkowski, J. *Global Fishery Resources of Tuna and Tuna-like Species*. (Food & Agriculture Org., 2007).
36. Pethybridge, H. *et al.* A global meta-analysis of marine predator nitrogen stable isotopes: Relationships between trophic structure and environmental conditions. *Glob. Ecol. Biogeogr.* **27**, 1043–1055 (2018).
37. Bird, C. S. *et al.* A global perspective on the trophic geography of sharks. *Nat. Ecol. Evol.* **2**, 299 (2018).
38. Houssard, P. *et al.* Trophic position increases with thermocline depth in yellowfin and bigeye tuna across the Western and Central Pacific Ocean. *Prog. Oceanogr.* **154**, 49–63 (2017).

39. Logan, J.M. *et al.* Lipid corrections in carbon and nitrogen stable isotope analyses: comparison of chemical extraction and modelling methods. *J. Anim. Ecol.* **77**, 838–846 (2008).
40. R Development Core Team. *R: a language and environment for statistical computing. R Foundation for statistical computing*. (2016).
41. Pinheiro, J. *et al.* Package 'nlme'. *Linear Nonlinear Mix. Eff. Models Version* 3–1 (2017).
42. McMahon, K. W., Ling Hamady, L. & Thorrold, S. R. A review of ecogeochemistry approaches to estimating movements of marine animals. *Limnol. Oceanogr.* **58**, 697–714 (2013).
43. Magozzi, S., Yool, A., Vander Zanden, H. B., Wunder, M. B. & Trueman, C. N. Using ocean models to predict spatial and temporal variation in marine carbon isotopes. *Ecosphere* **8**, e01763. 10.1002/ecs2.1763 (2017).
44. Cullen, J. T., Rosenthal, Y. & Falkowski, P. G. The effect of anthropogenic CO_2 on the carbon isotope composition of marine phytoplankton. *Limnol. Oceanogr.* **46**, 996–998 (2001).
45. Beardall, J. & Raven, J. A. Calcification and ocean acidification: new insights from the coccolithophore *Emiliania huxleyi*. *New Phytol.* **199**, 1–3 (2013).
46. Boller, A. J., Thomas, P. J., Cavanaugh, C. M. & Scott, K. M. Low stable carbon isotope fractionation by coccolithophore RubisCO. *Geochim. Cosmochim. Acta* **75**, 7200–7207 (2011).
47. Laws, E. A. Evaluation of in situ phytoplankton growth rates: A synthesis of data from varied approaches. *Annu. Rev. Mar. Sci.* **5**, 247–268 (2013).
48. Boyd, P. W. *et al.* Marine Phytoplankton Temperature versus Growth Responses from Polar to Tropical Waters – Outcome of a Scientific Community-Wide Study. *PLoS ONE* **8**, (2013).
49. Behrenfeld, M. J. *et al.* Climate-driven trends in contemporary ocean productivity. *Nature* **444**, 752–755 (2006).
50. Joo, H. *et al.* Long-Term Pattern of Primary Productivity in the East/Japan Sea Based on Ocean Color Data Derived from MODIS-Aqua. *Remote Sens.* **8**, 25 (2015).
51. Rousseaux, C. S. & Gregg, W. W. Forecasting Ocean Chlorophyll in the Equatorial Pacific. *Front. Mar. Sci.* **4**, (2017).
52. Karl, D. M., Bidigare, R. R. & Letelier, R. M. Long-term changes in plankton community structure and productivity in the North Pacific Subtropical Gyre: The domain shift hypothesis. *Deep Sea Res. Part II Top. Stud. Oceanogr.* **48**, 1449–1470 (2001).

53. Young, J. N., Bruggeman, J., Rickaby, R. E. M., Erez, J. & Conte, M. Evidence for changes in carbon isotopic fractionation by phytoplankton between 1960 and 2010. *Glob. Biogeochem. Cycles* **27**, 505–515 (2013).
54. Polovina, J. J., Howell, E. A. & Abecassis, M. Ocean's least productive waters are expanding. *Geophys. Res. Lett.* **35**, L03618 (2008).
55. Polovina, J. J. & Woodworth, P. A. Declines in phytoplankton cell size in the subtropical oceans estimated from satellite remotely-sensed temperature and chlorophyll, 1998–2007. *Deep Sea Res. Part II Top. Stud. Oceanogr.* **77–80**, 82–88 (2012).
56. McMahon, K. W., McCarthy, M. D., Sherwood, O. A., Larsen, T. & Guilderson, T. P. Millennial-scale plankton regime shifts in the subtropical North Pacific Ocean. *Science* **350**, 1530–1533 (2015).
57. Fry, B. & Wainright, S. C. Diatom sources of ^{13}C-rich carbon in marine food webs. *Mar. Ecol. Prog. Ser.* **76**, 149–157 (1991).
58. Tuerena, R. E. *et al.* Isotopic fractionation of carbon during uptake by phytoplankton across the South Atlantic subtropical convergence. (2019). doi:https://doi.org/10.5194/bg-2019-162
59. Rivero-Calle, S., Gnanadesikan, A., Castillo, C. E. D., Balch, W. M. & Guikema, S. D. Multidecadal increase in North Atlantic coccolithophores and the potential role of rising CO_2. *Science* **350**, 1533–1537 (2015).
60. Siegel, D. A. *et al.* Regional to global assessments of phytoplankton dynamics from the SeaWiFS mission. *Remote Sens. Environ.* **135**, 77–91 (2013).
61. Gregg, W. W., Rousseaux, C. S. & Franz, B. A. Global trends in ocean phytoplankton: a new assessment using revised ocean colour data. *Remote Sens. Lett.* **8**, 1102–1111 (2017).
62. Tagliabue, A. & Bopp, L. Towards understanding global variability in ocean carbon-13. *Glob. Biogeochem. Cycles* **22**, GB1025 (2008).
63. Cassar, N. & Laws, E. A. Potential contribution of β-carboxylases to photosynthetic carbon isotope fractionation in a marine diatom. *Phycologia* **46**, 307–314 (2007).
64. King, A. L. & Howard, W. R. Planktonic foraminiferal $\delta^{13}C$ records from Southern Ocean sediment traps: New estimates of the oceanic Suess effect. *Glob. Biogeochem. Cycles* **18**, (2004).
65. Gruber, N. *et al.* Spatiotemporal patterns of carbon-13 in the global surface oceans and the oceanic suess effect. *Glob. Biogeochem. Cycles* **13**, 307–335 (1999).

66. Olson, R. J. *et al.* Decadal diet shift in yellowfin tuna *Thunnus albacares* suggests broad-scale food web changes in the eastern tropical Pacific Ocean. *Mar. Ecol. Prog. Ser.* **497**, 157–178 (2014).
67. Quay, P., Sonnerup, R., Westby, T., Stutsman, J. & McNichol, A. Changes in the $^{13}C/^{12}C$ of dissolved inorganic carbon in the ocean as a tracer of anthropogenic CO_2 uptake. *Glob. Biogeochem. Cycles* **17**, 4-1-4–20 (2003).
68. Barnes, C., Sweeting, C. J., Jennings, S., Barry, J. T. & Polunin, N. V. C. Effect of temperature and ration size on carbon and nitrogen stable isotope trophic fractionation. *Funct. Ecol.* **21**, 356–362 (2007).
69. Deutsch, C. *et al.* Centennial changes in North Pacific anoxia linked to tropical trade winds. *Science* **345**, 665–668 (2014).
70. Somes, C. J. *et al.* Simulating the global distribution of nitrogen isotopes in the ocean. *Glob. Biogeochem. Cycles* **24**, GB4019 (2010).
71. Miloslavich, P. *et al.* Essential ocean variables for global sustained observations of biodiversity and ecosystem changes. *Glob. Change Biol.* **24**, 2416–2433 (2018).

9. Tables

Table1. Parameter and time-series data used to run various scenarios of imposed changes in phytoplankton dynamics, and the effects on the different spatial areas examined (New Caledonia Fiji (NC-Fiji) region, Pacific Ocean (PO), Atlantic Ocean (AO) and Indian Ocean (IO)). For example, $\delta^{13}C_{aq}$ explained 12% of the tuna $\delta^{13}C$ decrease $\Delta\delta^{13}C$, in 16 years in the PO, while an imposed 5% change in carbon fractionation factor (εf) explains 48% of $\Delta\delta^{13}C$, this factor having the largest sensitivity (1.53) compared to all factors tested (see methods for more details).

Factors (x)	starting value or equation used	sensitivity $\left(\frac{d\delta^{13}C_{tuna}}{\delta^{13}C_{tuna}}/\frac{dx}{x}\right)$	imposed change %	tuna $\Delta\delta^{13}C$, ‰, 16-yrs	% change explained			
					NC-Fiji	PO	AO	IO
$\delta^{13}C_{aq}$	Quay et al.[15]	-0.08	NA	0.30	14	12	22	38
CO_2	Cassar et al.[20]	0.21	NA	0.06	3	2	4	8
	Bidigare et al.[19]		NA	0.27	13	11	20	35
Growth rate (μ)	0.3	-0.2	-5	0.20	10	8	14	26
			-10	0.30	14	12	22	38
			-15	0.48	23	19	35	62
Carbon fixation fractionation factor (ε_f)	25	1.53	+1	0.24	12	10	17	31
			+2	0.48	23	19	35	61
			+3	0.72	35	29	52	92
			+5	1.20	58	48	87	154
b factor	120	-0.2	-2	0.10	5	4	7	13
			-4	0.20	10	8	14	26
			-8	0.40	19	16	29	51
			-10	0.50	24	20	36	64
Trophic fractionation factor (ε_{fc})	4	-0.23	-5	0.20	10	8	14	26
			-10	0.40	19	16	29	51
			-15	0.59	29	24	43	76

Table 2. Regression analysis output including the slope and intercept for each tuna species and ocean basin. Only one value is shown when similar for several species or oceans.

Ocean basin/Region	Tuna species	Intercept (in 2000)	Slope	Slope standard error	r^2	Temporal change (2000 to 2015, in ‰)	n
Atlantic	albacore	-17.4	-0.092	0.0085		-1.38	608
	bigeye	-16.6					126
	yellowfin	-16.6					256
Indian	albacore	-16.8	-0.052	0.0077	69.1	-0.78	248
	bigeye	-16.1					237
	yellowfin	-16.1					498
Pacific	albacore	-15.2	-0.166	0.0048		-2.49	878
	bigeye	-14.5					645
	yellowfin	-14.5					981
New Caledonia Fiji	albacore	-15.3	-0.138	0.0095	42.1	-2.07	364
	bigeye	-14.8					120
	yellowfin	-14.9					331
Global	all	-15.4	-0.120	0.0057	22.1	-1.80	4477

10. Figure captions

Figure 1. Map of global study area and locations of 4,477 samples for three tuna species. The black square delineates the New Caledonia-Fiji region used for a focused spatial and temporal analysis.

Figure 2. Time series of tuna muscle tissue $\delta^{13}C$ values (‰) with observations divided by ocean basin. The shaded area along the linear fit corresponds to a 95% confidence interval.

Figure 3. Predicted (color line) vs. observed (black line) changes in tuna muscle $\delta^{13}C$ values ($\Delta\delta^{13}C$, ‰) in the New Caledonia-Fiji region of the Pacific Ocean as a function of various processes. (a) The Suess effect. (b) Increase in CO_{2aq} in seawater under two scenarios based on different parametrizations in the literature (Bidigare et al.[21], Cassar et al.[22], see methods for details). (c) A decrease in phytoplankton cellular growth rate of 15%. (d) A change of 5% for the carbon fractionation factor ε_f and 10% for the constant b used to calculate carbon isotope fractionation during photosynthesis (see methods for details), and also all factors considered together, except growth rate (blue line = Suess effect + CO_{2aq} from Bidigare et al.[21] + b + ε_f).

Figure 4. Synthesis of the potential effects of various factors on the tuna $\delta^{13}C$ temporal trend ($\Delta\delta^{13}C$). Different combinations are possible (see text for more details). Tuna illustration Les Hata ©SPC.

Author information

Contributions

A.L, A.R., N.C and H.P analyzed the data and interpreted the results with the help of B.F. A.R. and D.E.P. performed the statistical analysis. A.L, N.C and H.P wrote the manuscript with the help of A.J.H. and A.R. All authors contributed to and provided feedback on various drafts of the paper.

Competing interests

The authors declare no competing interests.

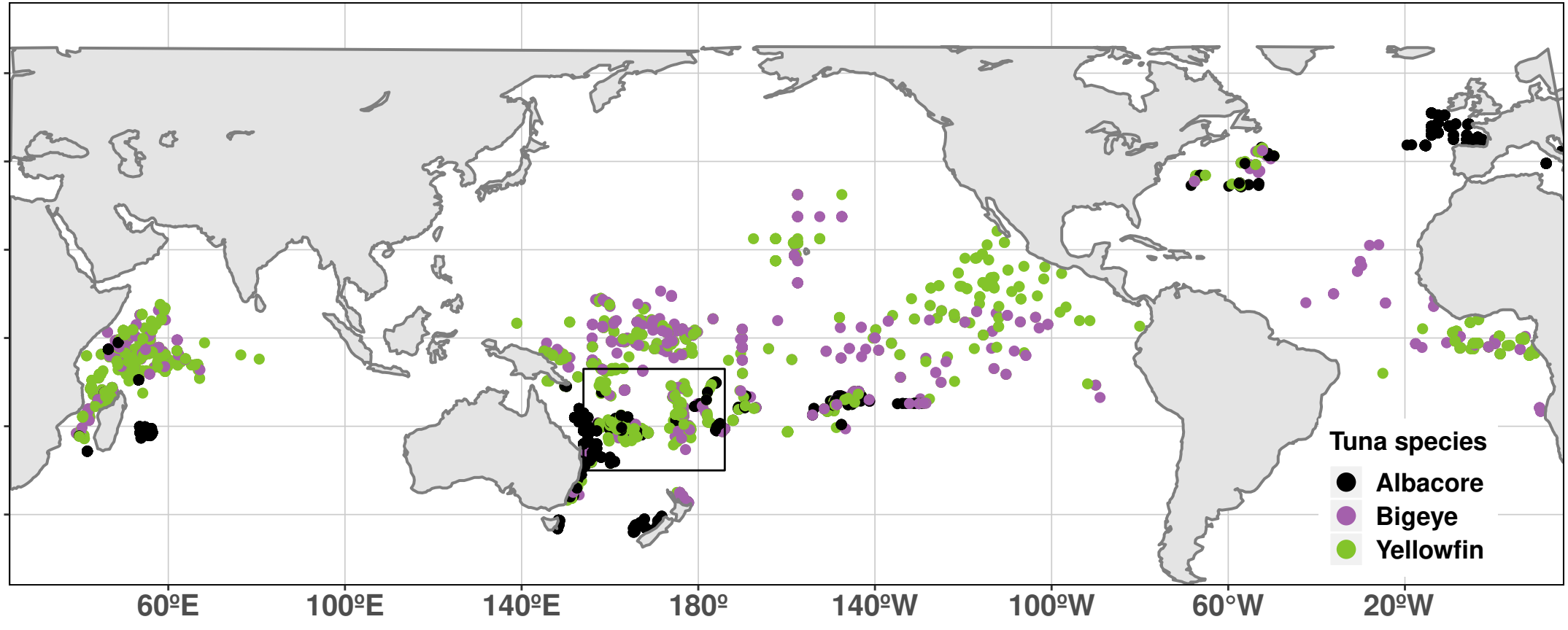

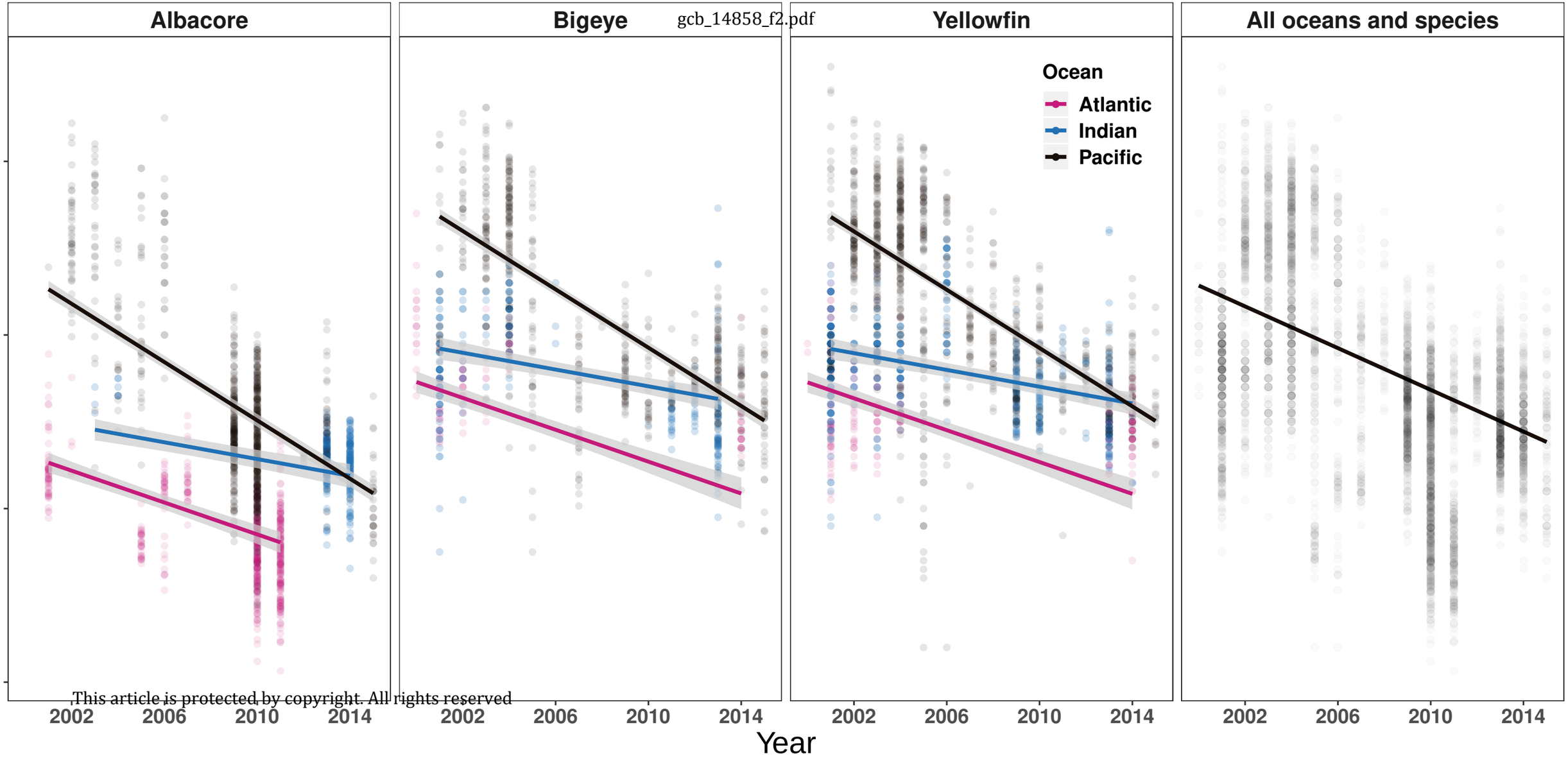

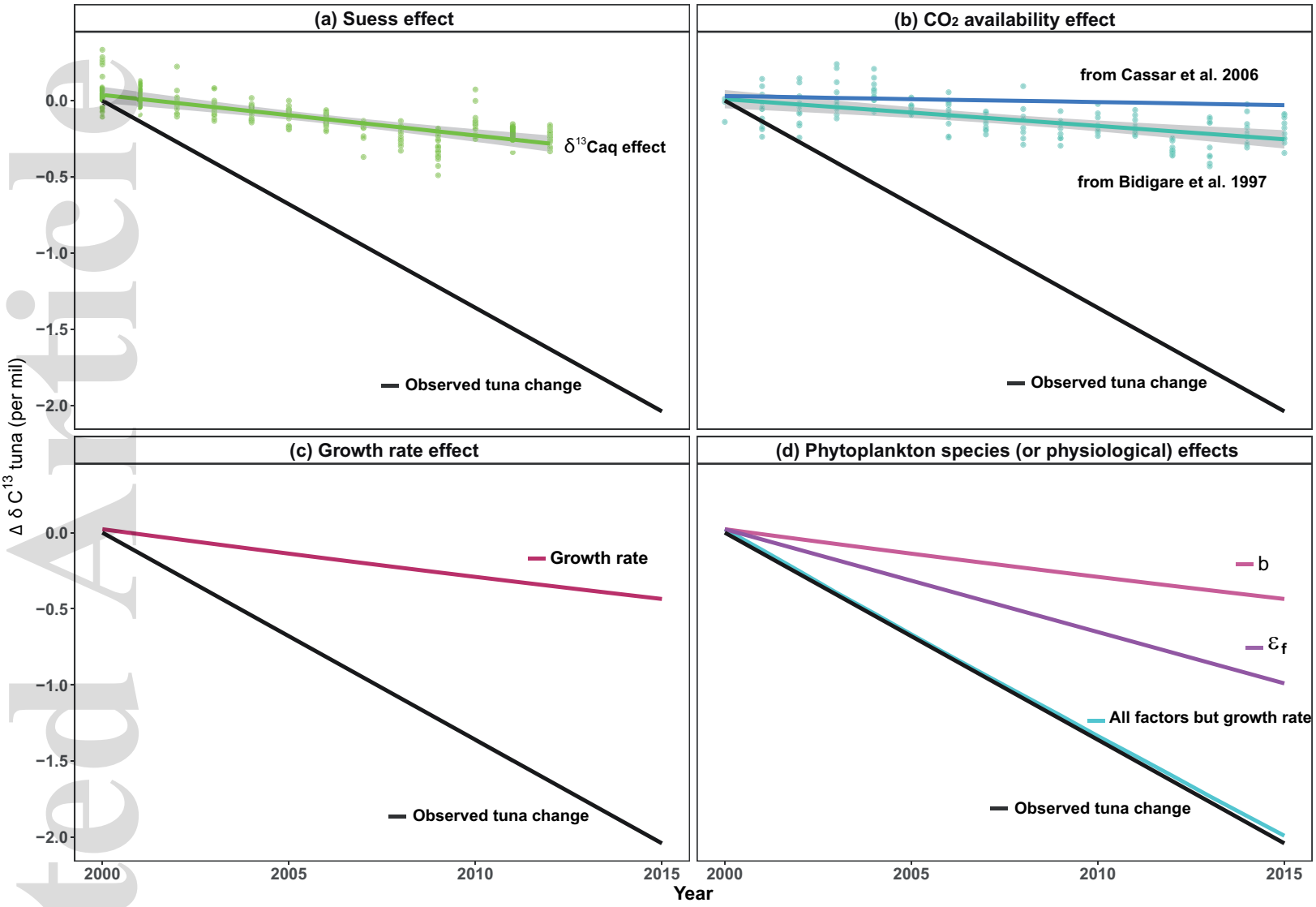

gcb_14858_f3.eps

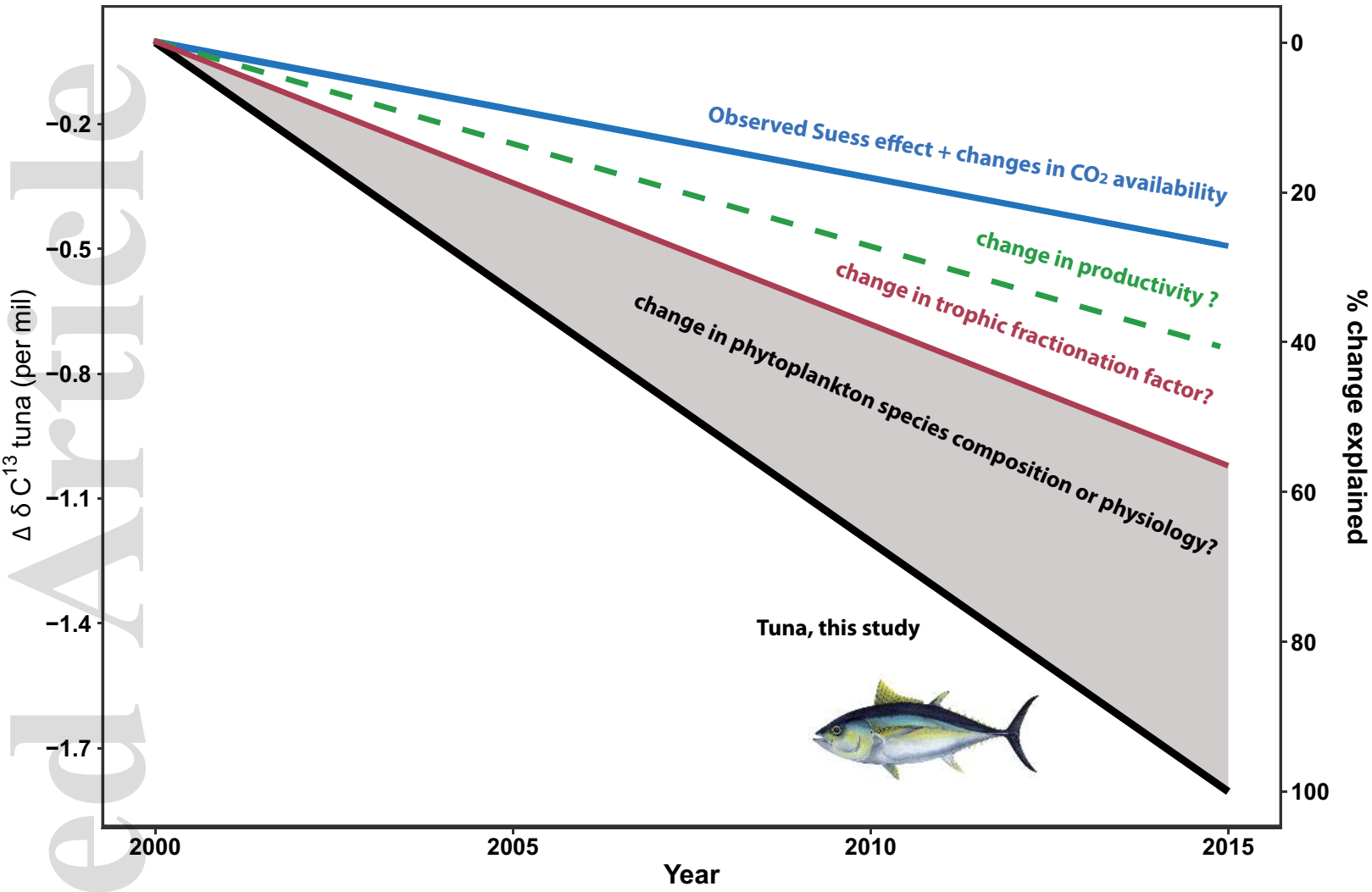

gcb_14858_f4.eps